D. Applications

1. Single Component Model

The major accomplishments are:

- Identified the important parameters and estimated their effect on reactor performance.
- Estimated the effect of axial mixing and catalyst settling on reactor performance.
- Determined operating conditions which yield maximum utilization of bubble-column reactor volume for bench-scale unit.

a. Estimation of Kinetic Constants for Fischer-Tropsch Reactions

Kinetic constants are essential parameters for the slurry F-T reaction mathematical models. Some effort was spent to estimate the constants based on the published experimental data in slurry F-T operations. Data from five sources were used (Koelbel, et al. (1955), Koelbel and Ralek (1980), Schlesinger, et al. (1954), Mitra and Roy (1963), and Kunugi, et al. (1968)). All data were based on bubble-column operations since no data from other slurry reactor types were found at the time.

Since data from bubble-columns contain both mass transfer and kinetic effects, the estimated kinetic constants depend strongly on the assumptions used to describe the mass trasnfer phenomenon. All the data, except that from Koelbel, et al. (1955), were obtained from long and slim bubble-columns. Hence, it is expected that the effect due to liquid-phase axial dispersion is very small. Therefore, it was decided to use a model of Non-Mixing liquid phase in treating these data. This approach is similar to that used by Deckwer, et al. (1981). Basically the model assumptions are the same as those described in Section IV.B. In addition, it was assumed that the catalyst is uniformly distributed in the reactor.

The experimental data from the five sources, all on Fe-base catalysts, are summarized in Table 29 and the estimated kinetic constants are given in Table 30. There the kinetic resistances as percentages of the total resistances are also given. These are defined as

$$R_k/(R_k+R_d)$$

where R_k and R_d are, respectively, the kinetic resistance for H_2 conversion and the H_2 diffusional resistance from the gas-liquid interface to the bulk liquid (see Figure 35). In Section VII.B,

Table 29

Selected F-T Conversion Data in Bubble-Column Reactors

Authors	Catalyst	Temp. (°C)	Pressure (MPa)	Reactor Dimension d_R(cm) x L(cm)	Superficial Inlet Gas Velocity (cm/s)	Inlet H_2/CO	Hydrogen Conversion	H_2/CO Usage Ratio	Catalyst Loading (Wt %)
Koelbel, et al. (1955)	Pptd Fe	268	1.2	129 X 770	9.5	0.67	86	0.63	28.4
Koelbel and Ralek, (1980)	Pptd Fe	266	1.1	4.7 X 350	3.5	0.67	85	0.65	15.4
Schlesinger, et al. (1954)	Fused Fe	258	2.17	7.6 X 305	1.54	1.0	63.9	0.81	21.1
Mitra and Roy (1963)	Fe pptd on Kieselgur	260	1.13	5.1 X 305	1.48	1.33	89.7	1.27	17.0
Kunugi, et al. (1968)	Pptd Fe	266	1.12	5.0 X 550	3.78	0.59	80.8	0.59	4.6

Table 30

Estimated F-T Kinetic Constants on Fe-Catalysts

(Non-Mixing Liquid Phase Single-Component Model)

Authors	Temperature (°C)	k''_H [1]	Kinetic Resistance as % of Total Resistance
Koelbel, et al. (1955)	268	0.931	0.92
Koelbel and Ralek (1980)	266	1.12	0.80
Schlesinger, et al. (1954)	258	0.203	0.84
Mitra and Roy (1963)	260	0.848	0.68
Kunugi, et al. (1968)	266	2.28	.89

[1] Intrinsic kinetic rate constant defined as $r_H/(1-\epsilon_g)(1-v_c)C_{HL}C_{Fe}$, ($cm^3$ liquid/s-gFe).

it was shown that these two are the only important resistances among the six steps attributed to the transfer of H_2 from the gas phase to the catalyst and to the H_2 conversion on the catalyst.

The same five sets of data were evaluated by Deckwer, et al. (1981a) for the kinetic constants. They report rate constant values which are very similar to those reported on Table 30 except that the values from the first two and the last sources are about 7% less than the corresponding values from Deckwer, et al. (1981a). This small discrepancy is probably due to their assumptions that the H_2/CO usage ratio is the same as the inlet H_2/CO ratio and that the H_2 conversion is the same as the H_2+CO conversion.

By comparing the intrinsic kinetic rate constants, k_H", given in Table 30, the following conclusions can be drawn:

- The catalysts from Koelbel, et al. (1955), Koelbel and Ralek (1980), and Mitra and Roy (1963) have catalytic activity within the range 0.85-1.1 cm^3 liquid/s-gFe.
- The catalyst used by Kunugi, et al. (1968) is about 2.3 times more active than those mentioned above.
- The fused-iron catalyst used by Schlesinger, et al. (1954) has a relatively low activity level.
- The kinetic resistance is much larger than the corresponding diffusional resistance provided the gas bubble size is sufficiently small (in this study, d_B = 0.7 mm).

Among the five sets of bubble-column data, the first set by Koelbel, et al. (1955) was obtained in a large reactor (1.29 m ID). Since a large reactor may result in a substantial axial dispersion due to the relatively free movement of the liquid, the data must be examined more closely. Table 31 shows the estimated intrinsic rate constants obtained by using the three different liquid-phase mixing models: non-mixed (NM), perfectly mixed (PM) and axially dispersed (AD). The predicted rate constant from the PM model is more than double that from the NM model. However, using liquid phase mixing correlations from the literature and the AD model results in only a 2-10% increase in the rate constant over that predicted by the NM model.

A k_H" of 1.1 cm^3 liquid/gFe-s at a nominal temperature of 266°C is recommended for a precipitated Fe-type catalyst. This value is based on data obtained by Koelbel and Ralek (1980) in bench-scale bubble-column and will be used at base case for current calculations.

Table 31

Estimated Kinetic Rate Constants Using
Different Liquid-Phase Mixing Single-Component Models[1]

Intrinsic Kinetic Rate Constant	Liquid-Phase Axial Mixing Models		
	Non-Mixing	With Axial Mixing	Perfectly-Mixed
k_H''	.93	.95[2]	2.09

(1) Rheinspressen-Koppers Demonstration Plant data from Koelbel and Ralek (1980).

(2) This value is based on using the equivalent hydraulic diameter (25.4 cm) as the effective reactor diameter. Using the free-flow area diameter as the effective reactor diameter gives a value of 1.02.

b. Parametric Study

The results of the parametric study show:

- An active catalyst is essential if high synthesis gas conversion is to be obtained with a reasonable reactor height.
- With a plug-flow gas phase, perfect mixing in the liquid phase will substantially increase the reactor height required to achieve high synthesis gas conversion.
- The effect of molar contraction during the F-T reaction on the synthesis gas concentration is large, and should be included in the mathematical model.
- The size of bubbles in the slurry reactor has to be maintained small to reduce the mass transfer resistance and achieve high synthesis gas conversion.

Other major effects (axial dispersion, catalyst settling, and optimal gas velocity) are discussed in subsequent subsections. The base case parameters used in calculations are those given in Table 26.

Figure 37 shows the effect of kinetic rate and liquid phase mixing on H_2 conversion. It is essential to have a very active catalyst to obtain high conversion within a reasonable reactor height. The liquid phase mixing has a large effect on the required reactor length within the high conversion region. It is expected that the bubble-column reactor in the bench-scale pilot plant will have limited liquid phase mixing and that its performance will fall between the Non-Mixing case and the Perfectly-Mixed case. Nevertheless, unless the catalyst is extremely active, a large reactor height is necessary to achieve high conversion.

F-T synthesis reaction is accompanied by a decrease in total number of moles. This molar contraction during the reaction will have two effects on the model formulation:

- changing the concentration of the reactants when the conversion increases
- changing the hydrodynamic properties, such as the superficial gas velocity, the bubble size, the gas holdup, and the gas-liquid interfacial area, along the reactor

FIGURE 37

EFFECT OF KINETIC RATE AND LIQUID PHASE MIXING ON H_2 CONVERSION

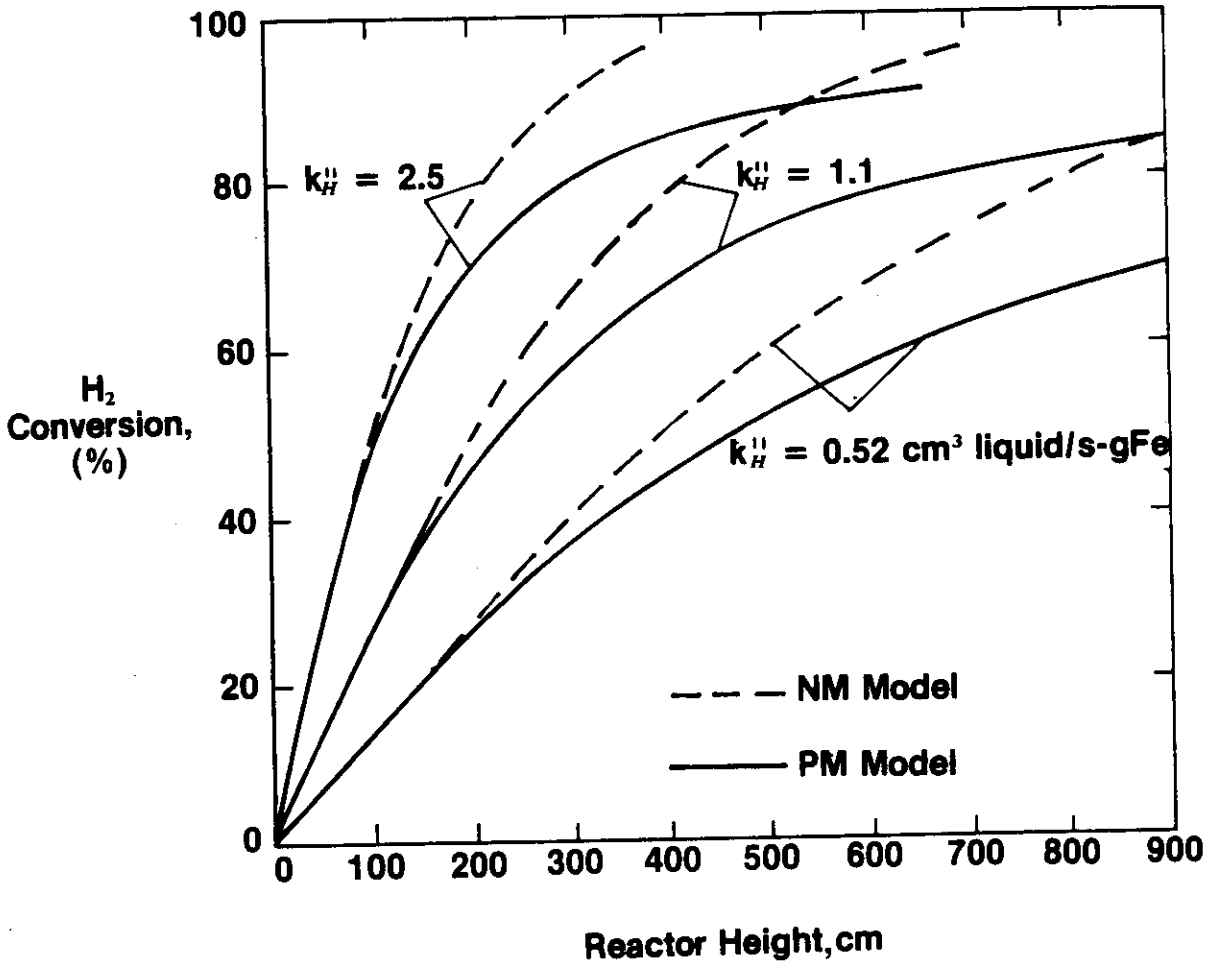

Figure 38 shows the effect of molar contraction during the F-T reaction on the H_2 conversion. Only the effect of the molar contraction on the changing reactant concentration is taken into account here. The comparison is with the case assuming no molar change during reaction. The result shows that the reactor height required is about 30% less at high syngas conversion in the case with 50% molar contraction than that with no molar change. It is important to include this effect of molar contraction in the mathematical model.

Figure 39 shows the effect of bubble size on H_2 conversion. Bubble size has a very large effect on column performance. It is extremely important to have small gas bubbles. The same figure also shows the result of infinite catalytic activity. At infinite catalytic activity, the only resistance to H_2 conversion is the diffusion from the gas-liquid interface to the bulk liquid phase. In other words, this is the best one can do by raising the catalyst conversion activity level.

The effect of the changing hydrodynamic properties along the reactor on the reactor performance is rather complicated. The changing gas-liquid interfacial area (a_g) and gas holdup (ϵ_g) affect both the gas-liquid interface to bulk-liquid transfer resistance (R_d) and the kinetic resistance (R_k). To thoroughly examine this effect, calculations on the following four cases were done:

Cases	u_g in $\epsilon_g=0.053(u_g)^{1.1}$	Bubble Size	Remarks
1	u_g	Constant	Present base case (constant ϵ_g and a_g)
2	u_{gm}	Constant	Constant ϵ_g and a_g
3	$u_g(z)$	Constant	Variable ϵ_g and a_g
4	$u_g(z)$	Variable	Variable ϵ_g and a_g, but constant number of bubbles

where u_{gm} is the arithmetic average of the inlet and outlet gas superficial velocities.

The equations and the solution for Cases 1 and 2 are given in Section VI.C. In Cases 3 and 4, both the gas holdup and the gas-liquid interfacial area vary with the H_2 conversion. An analytical solution is not available. A method of numerical integration, i.e., trapezoidal quadrature, was used to integrate the resulting differential equation.

Calculations illustrating the effect of variations of hydrodynamic parameters on bubble-column performance are shown in Figure 40 for the case of Non-Mixing liquid phase. For k_H"=1.1 cm^3 liquid/s-gFe, the differences in model predictions are small

FIGURE 38

EFFECT OF MOLAR CONTRACTION DURING REACTION ON H_2 CONVERSION

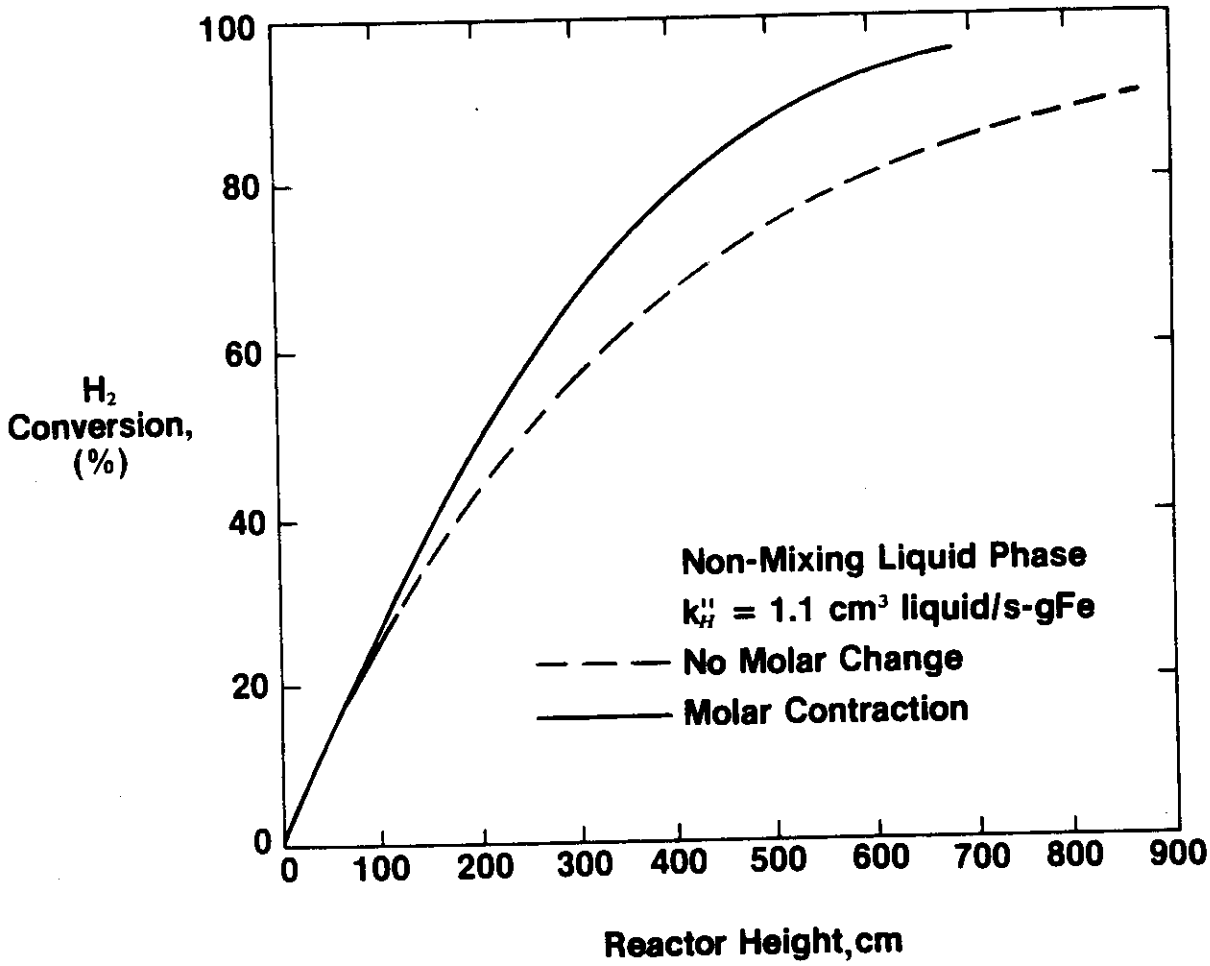

FIGURE 39

EFFECT OF BUBBLE SIZE ON H_2 CONVERSION

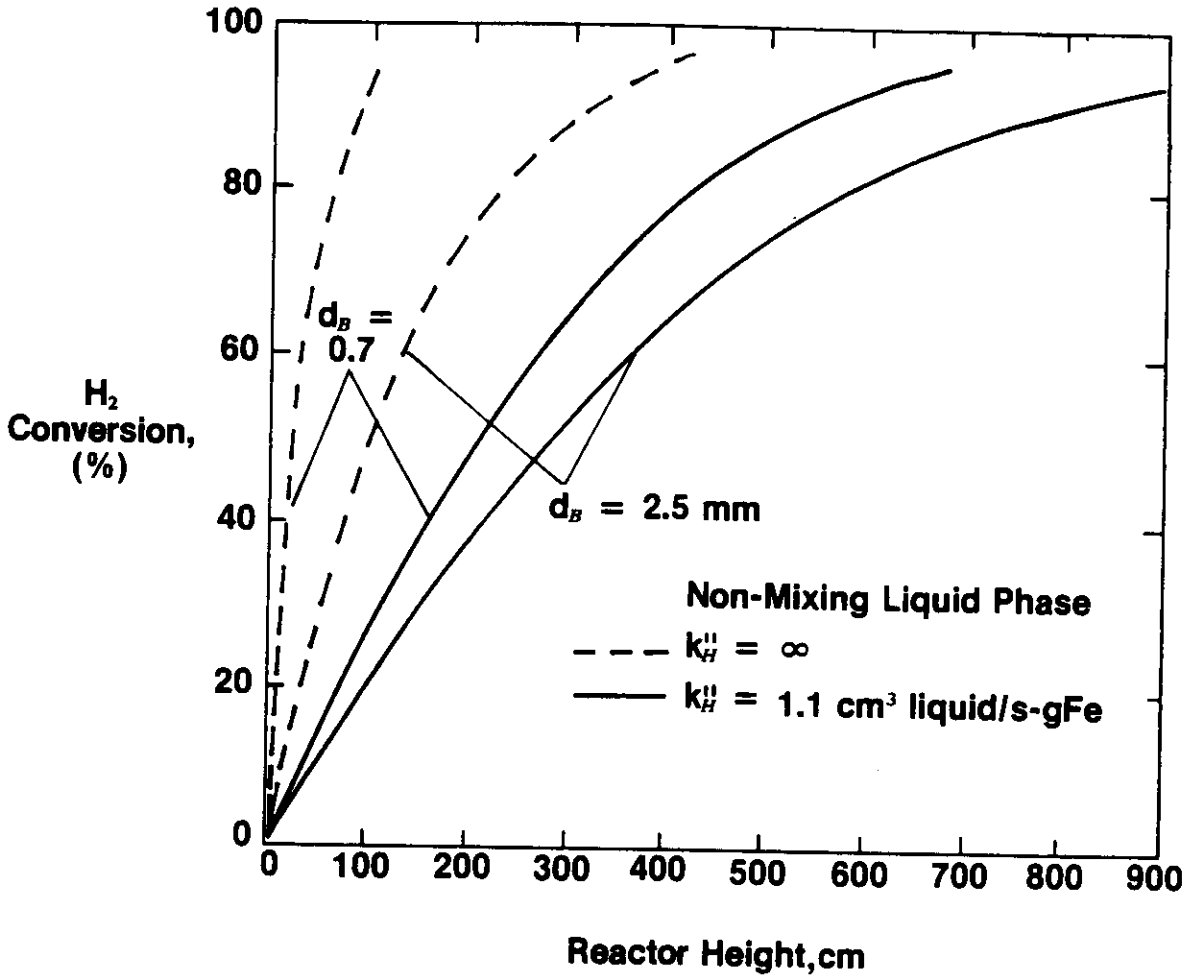

FIGURE 40

EFFECT OF HYDRODYNAMIC PARAMAETERS ON H_2 CONVERSION

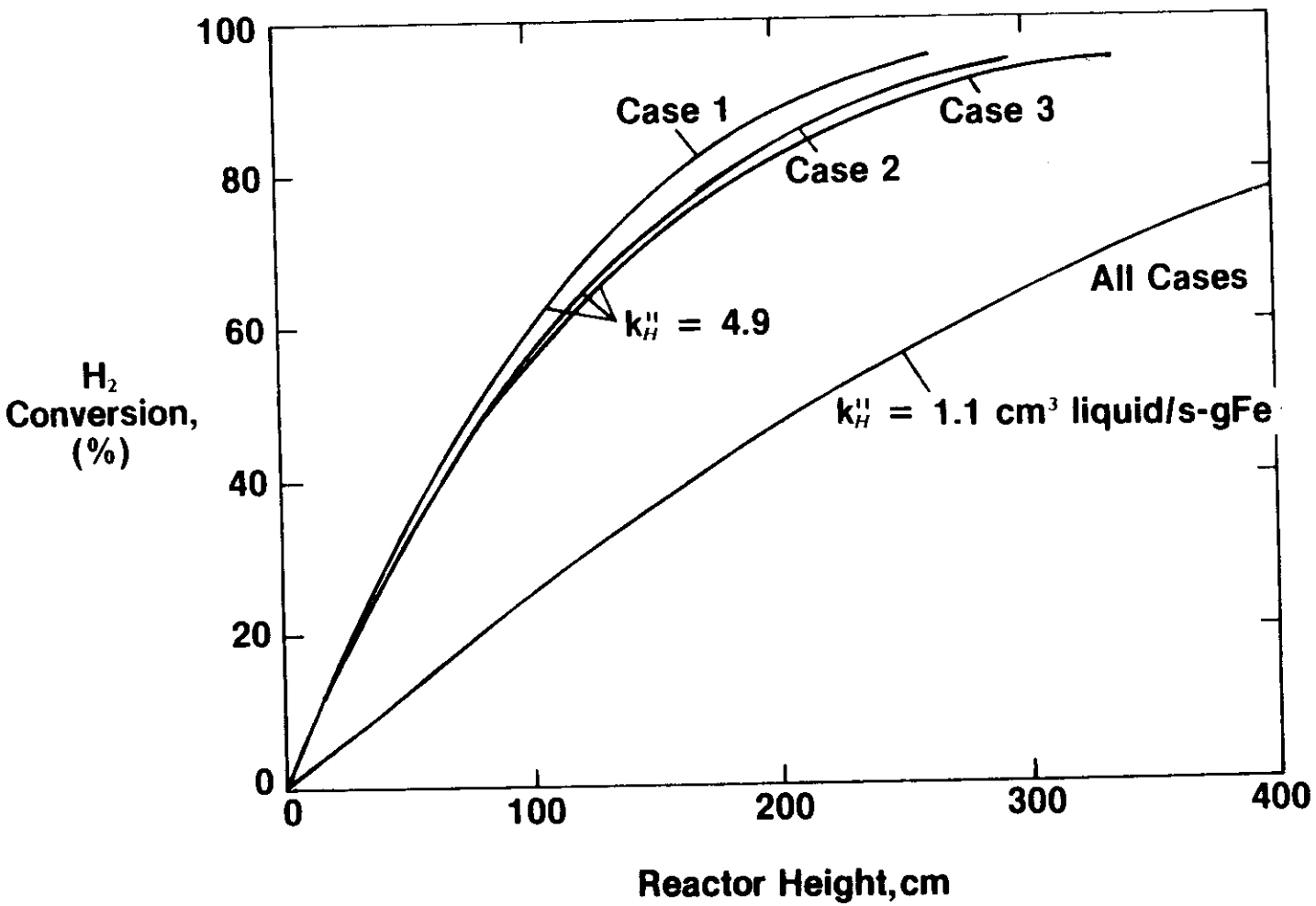

and the results for all four cases can be represented by a single curve. For k_H"=4.9 cm^3 liquid/s-gFe, three curves, corresponding to Cases 1, 2 and 3, are shown in Figure 40. The results obtained for Case 4 fall very close to that of Case 2 and are not shown. Although the deviation between Cases 1 and 3 are quite significant, there is very small deviation between Cases 2 and 3. Consequently, the use of the average gas holdup and gas liquid interfacial area is sufficient to describe the changing hydrodynamic properties along the reactor resulting from the molar contraction of the F-T reaction.

The effect of the changing hydrodynamic properties on the H_2 conversion in the case of the Perfectly-Mixed liquid phase was evaluated similarly . The differences in results between all four cases are smaller than those between the corresponding cases of the NM model.

The mathematical model, as illustrated by Case 2, using a constant bubble size and the mean value of the gas holdup, gives adequate results for catalysts of activity level less than k_H"=4.9 cm^3 liquid/s-gFe.

c. Effect of Catalyst Settling on Reactor Performance

In the F-T slurry process, fine catalyst particles are suspended in the liquid phase by the bubbling of the syngas. This uplifting force is balanced by the gravitational force on the particles. Therefore, the axial catalyst distribution is generally non-uniform. This non-uniform catalyst distribution will lower reactor performance. The objective here is to evaluate this effect on BSU F-T reactor performance using a catalyst dispersion model coupled with the slurry F-T reactor mathematical model described in Section VII.C. Specifically, the most important variable that affects catalyst distribution is the catalyst size. If the size is small enough, the axial catalyst distribution will be relatively uniform and good reactor performance can be ensured. The primary objective of this study is to determine the maximum catalyst size such that the deviation of reactor performance due to non-uniform axial catalyst distribution will not be significant. Furthermore, Farley and Ray (1964), Schlesinger, et al. (1954), and Koelbel and Ralek (1980) reported that F-T Fe-based catalysts disintegrate during normal operation. The former two reported that catalysts disintegrate to 1-3μm size. A secondary objective of this study is to establish that such stabilized catalyst size is small enough for proper operation. It is expected that satisfying the primary objective will automatically accomplish this. For the present study, the NM liquid phase mathematical model is used (Equation (19)). Table 32 gives the values of the parameters used in the calculations.

Table 32

Parameters and Their Ranges Adopted in Single-Component F-T Reactor Mathematical Model Calculations

Parameters	Base Case	Ranges
Hydrodynamic Parameters		
d_B, (cm)	.07	.07-.25
k_L, (cm/s)	.02	.02-.09
ϵ_g	$.053(u_{gm})^{1.1}$	$(.053-.106)(u_{gm})^{1.1}$
Reaction Parameters		
k_H'', (cm^3 Liquid/s-gFe)	1.1	.5-2.0
U	.645	.6-.69
$-\alpha$	.5	.5-.6
Physical Parameters		
D_{HL}, (cm^2/s)	10^{-4}	10^{-4}-10^{-3}
f_{Fe}	.67	-
K_H (cm^3 Liquid/cm^3 Gas)	4.4	2.2-6.6
ρ_L, (g/cm^3)	.667	-
ρ_s, (g/cm^3)	5.2	-
μ_L, (g/s-cm)	.022	-
Operation Parameters		
d_R, (cm)	5.08	5.08-1.29
f	.7	.6-.7
P, (MPa)	1.48	-
T, (^oC)	265	-
u_g^i, (cm/s)	4	2-9.5
wf_{Fe}	.10	.05-.20

A parametric study of this axial catalyst dispersion effect shows that the deviation of the F-T bubble-column reactor performance from that with a uniform catalyst distribution is the largest when:

1. The catalyst loading is low.

2. The feed gas superficial velocity is high.

Consequently, to study the same effect on the BSU F-T reactor performance, the maximum deviation is expected at the lowest catalyst loading of about 5 wt % Fe and the highest feed-gas superficial velocity of about 7 cm/s. The effect of a non-uniform catalyst distribution can be represented as the percentage increase in reactor length required to achieve the same hydrogen conversion as that estimated using a uniform catalyst distribution. These results are given in Figure 41 with catalyst sizes from 10 to 50μm. If one considers that a 15% longer reactor length is an acceptable deviation, then the acceptable catalyst size is below 40μm for 90% hydrogen conversion.

In open literature, many sizes of the fresh Fe-based catalysts have been mentioned. However, the slurry reactor diameters and the feed-gas superficial velocities are not exactly those used in the current study. Koelbel and Ralek (1980) mentioned a 30μm catalyst for a 5.1 cm diameter bench-scale unit at a 3.5 cm/s feed-gas superficial velocity, and the same size catalyst for the Rheinsprussen demonstration plant (1.29m reactor and 9.5 cm/s feed-gas superficial velocity). Schlesinger, et al. (1951) used catalyst smaller than 60μm for a 7.6 cm diameter reactor and a feed-gas superficial velocity of about 2.5 cm/s. Sakai and Kunugi (1974) used a 1μm catalyst for a 5.1 cm diameter reactor and a 3.8 cm/s feed-gas superficial velocity.

As mentioned in the first paragraph of this subsection, catalyst disintegration to sizes below 5μm may be expected during normal operation. Since this size is much smaller than the 40μm limit recommended for the fresh catalyst, no operational difficulties due to catalyst non-uniform distribution are expected.

d. Optimum Reactor Space-Time Yield

One of the questions often raised in the discussion of the F-T reactor performance is the possible disadvantage due to the inherently low catalyst density in slurry reactors. In other words, it requires a larger reactor volume to hold the same amount of catalyst than the conventional vapor-phase F-T reactors. This larger reactor volume may pose a penalty as a higher cost for the final product. Consequently, it is important to examine the Space-Time-Yield behavior of a F-T slurry reactor

FIGURE 41

EFFECT OF AXIAL CATALYST DISTRIBUTION ON BSU F-T REACTOR PERFORMANCE

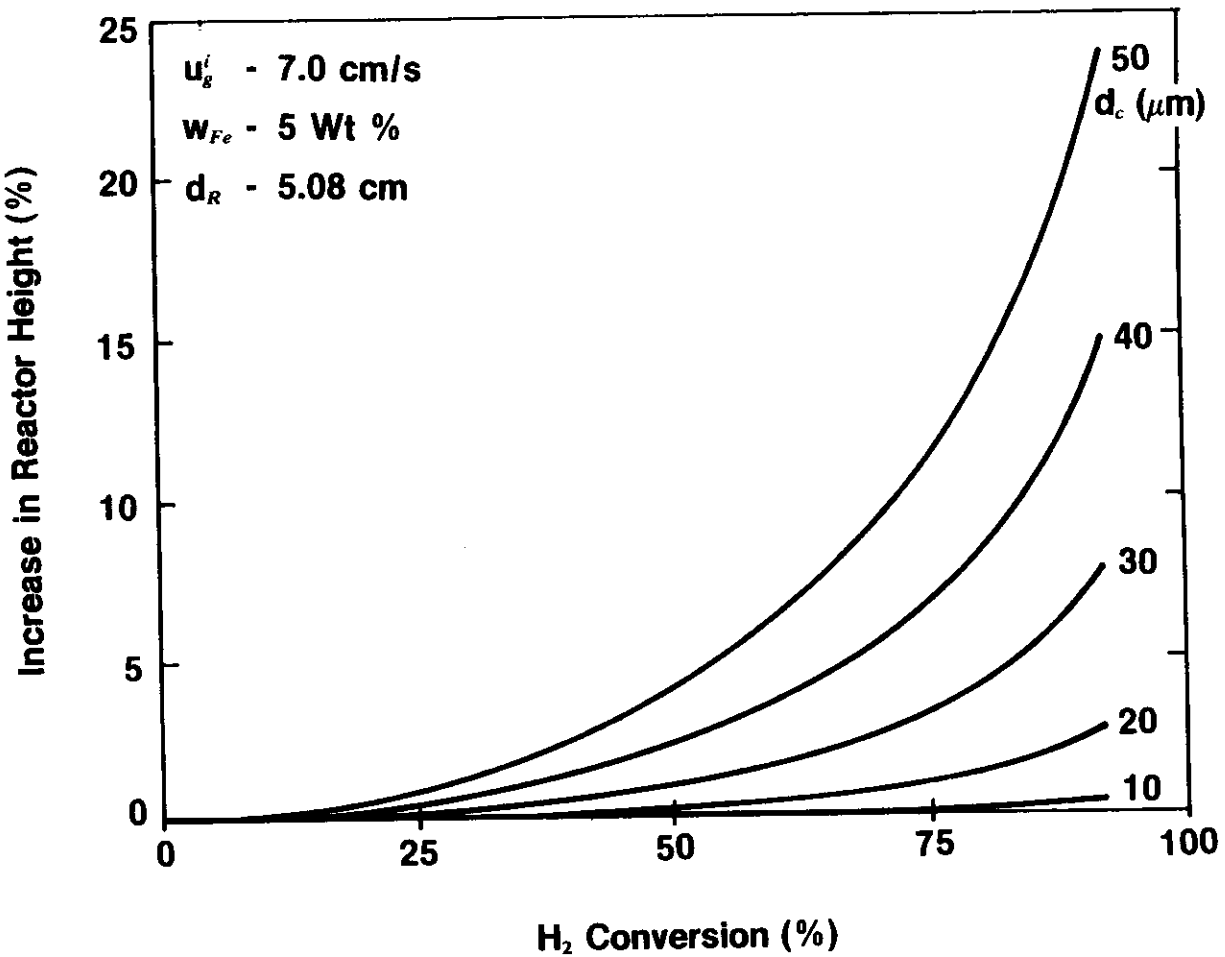

in order to search for an optimal STY operation. The Space-Time-Yield used here is defined as:

$$STY = (gMol\ H_2+CO\ Converted/hr\text{-}cm^3\ Expanded\ Slurry) \qquad (38)$$

Based on the current mathematical model, the yield is strongly dependent on the catalyst loading and the gas velocity. Using the NM mathematical model, Figure 42 shows results of calculations for the BSU F-T reactor operation. Only the results for the 90% hydrogen conversion are given. As expected, the STY depends strongly on the catalyst loading. Note that, in the current mathematical model, the hydrodynamic properties of the column are assumed to be independent of the catalyst loading. Deckwer, et al. (1982b) mentioned that this independence exists up to 16 wt % of catalyst in the slurry. However, Koelbel and Ralek (1980) indicated that the optimum catalyst loading is about 10 wt % in terms of the iron in the slurry. Higher catalyst loading increases the viscosity of the slurry and thus decreases the gas-liquid interfacial surface area. Based on these two references, the question of the optimal catalyst loading will need further investigation. The calculated results for the high catalyst loadings shown in Figure 42 can only be used as a guide for future studies.

The dependence of the STY on the gas velocity is very interesting because maximum STY's exist for each curve. The physical interpretation of this phenomenon is that, at low gas velocity, the STY is low because the gas-liquid interfacial surface area is low; while, at high gas velocity, the STY also is lower because the slurry-bed expansion becomes an overriding factor. In Figure 42, a dotted line indicates the locus of the maximum STY. For catalyst loadings between 5-15 wt % Fe, the feed gas superficial velocities at which the maximum STY occurs vary from 2.8 to 4.6 cm/s. Caution should be given in interpreting the results at the high end of the gas velocity, since, according to Deckwer, et al. (1982a), the flow in the BSU F-T column may approach "slug flow" regime at about 8 cm/s gas velocity.

e. Effect of Liquid-Phase Axial Mixing

Calculations in Subsection VII.D.1.b have shown that the state of the liquid phase axial mixing has a large effect on slurry F-T reactor performance. That conclusion was drawn by using two extreme states of the liquid phase mixing, i.e., non-mixing (NM model) and perfect-mixing (PM model). The actual state of the axial liquid mixing lies somewhere between these two extremes. The purpose of this work is to investigate the effect of this liquid phase axial dispersion on BSU F-T reactor performance using a physical model similar to the one adopted by Deckwer, et al. (1982b) in which an axial dispersion coefficient is used (Equations (14), (17), and (18)).

FIGURE 42

EFFECT OF CATALYST LOADING AND GAS VELOCITY
ON BSU F-T REACTOR PERFORMANCE

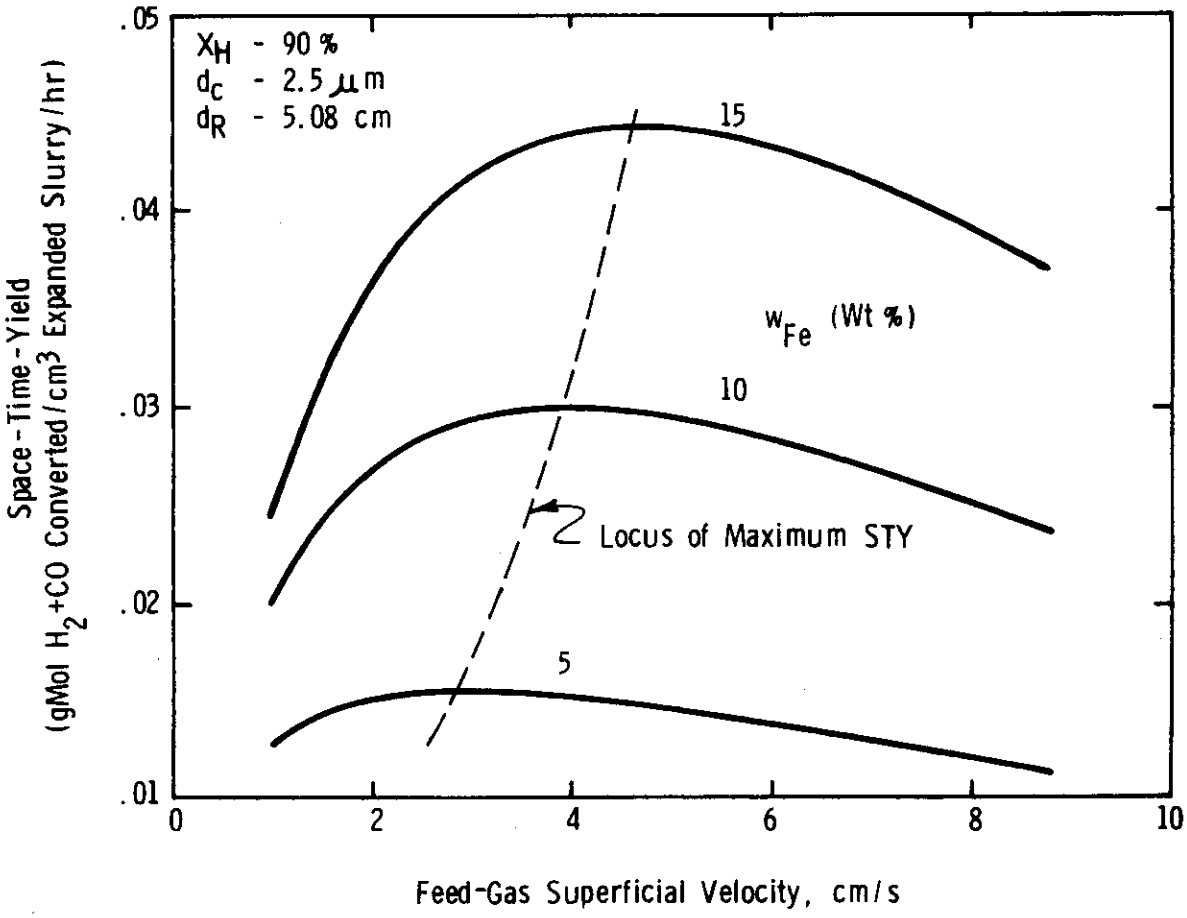

The major results of the calculations are:

- The effect of the liquid-phase axial mixing on the BSU F-T reactor performance is estimated to be small to moderate.

- The effect of the liquid-phase axial mixing on large-scale F-T bubble reactor performance can be significant. However, this effect is greatly complicated by the existence of cooling tubes in large-scale reactors. Further experimentation to evaluate the hydrodynamic behavior of large-scale reactors is recommended.

Table 32 lists the parameters adopted in the current mathematical model calculations. To evaluate the effect on the reactor performance due to the axial liquid-phase mixing, a parametric study was done to find out the effect of major parameters on the directional change in the reactor performance. This exercise is essential in establishing a combination of parameters that will give the largest effect on the reactor performance due to the axial liquid-phase mixing. If this case shows a small effect, then it can be concluded that the effect is small in all cases enveloped by the ranges of the parameters under consideration. There are two types of perturbation of these parameters. One type results from the variation within the operational range of parameters, such as the reactor temperature, reactor pressure, catalyst loading, inlet H_2/CO ratio, superficial feed-gas velocity, and reactor diameter. The other type is the variation of the parameters due to the uncertainty of these parameters, such as the gas bubble size, gas holdup, hydrogen solubility, hydrogen diffusivity, intrinsic kinetic rate constant, H_2/CO usage ratio, and contraction factor. All parameters listed in Table 32 are subjected to parametric study except for the Fe-content in the catalyst, catalyst solid density, liquid density and viscosity, reactor pressure, and reactor temperature. The variations of the liquid density and viscosity are reflected in the variation of the liquid-side mass transfer coefficient. Finally, the variation of the reactor temperature is mainly reflected in the variation of the intrinsic kinetic rate constant; while the variation of the reactor pressure is reflected in the variation of the gas velocity.

The base case values of the parameters are given in Table 32 together with the ranges of the variations of each parameter. The lower and upper bounds of the gas bubble diameter are those reported by Deckwer, et al. (1982b) and Satterfield and Huff (1980). Those for the liquid-phase hydrogen diffusivity are obtained from the Wilke-Chang correlation (Deckwer, et al. (1982b) and Calderbank, et al. (1963)). Those for the hydrogen solubility coefficient and the intrinsic kinetic

constant are obtained by varying the base case value by ±50%. Those for the contraction factor are those measured by Deckwer, et al. (1982b). Those for the H_2/CO usage ratio are given arbitrarily but within a reasonable limit. Lastly, the upper bound of the gas holdup is obtained by doubling the base case value.

The liquid-phase axial mixing is described using a constant dispersion coefficient. A correlation for this coefficient recommended by Deckwer, et al. (1982b) is adopted here (Table 27). The correlation includes data obtained with the superficial gas velocity up to 90 cm/s and with the reactor diameter up to 60 cm. Some of these data may very well be in the turbulent flow region. However, most of the data were obtained in systems of air-water, and some were in systems of air-aqueous glycerine. It is not clear if data obtained from these systems can be applied to our present system. In the current study, the calculated effect of the liquid-phase axial mixing on the F-T bubble-column performance is compared against those of the Non-Mixing (E_L=0) and the Perfectly-Mixed (E_L=∞) cases.

Table 33 summarizes results of this parametric study. It shows the variations of the parameters that result in an increase in calculated effect on the F-T bubble-column performance due to the existence of the liquid-phase axial mixing. An increase in this effect is measured by an increase of the following parameter

$$(1-X_H^e)_{AD}/(1-X_H^e)_{NM}$$

where the subscript AD denotes the case with the existence of the liquid-phase axial dispersion and the subscript NM denotes the case of non-mixing liquid-phase. In conclusion, to obtain a case that gives the largest effect due to the existence of the liquid-phase axial dispersion, one shall use the upper-ranged values of the liquid side mass transfer coefficient, intrinsic kinetic rate constant, H_2/CO usage ratio, contraction factor, liquid-phase hydrogen diffusivity, catalyst loading in the reactor slurry, reactor diameter, and lower-ranged values of the gas bubble size, gas holdup, hydrogen solubility coefficient, superficial feed-gas superficial velocity, and inlet H_2/CO ratio. If the predicted effect of this case of largest liquid-phase axial dispersion is small, then one can conclude that the effect is small for all cases within the ranges of the parameters.

The effect of the liquid-phase axial mixing on the BSU F-T reactor performance can now be estimated using the largest effect case at 5.1 cm reactor diameter. The result of this calculation is plotted in Figure 43, given as the hydrogen conversion versus the reactor length. For comparison, the results for both the non-mixing and the perfectly-mixed liquid cases are plotted in the same diagram. The curve representing

Table 33

Variation of Parameters That Results in an Increase of the Calculated Effect of the Liquid-Phase Axial Mixing on the F-T Bubble-Column Performance

Parameters	Variation[1]	Parameters	Variation[1]
Hydrodynamic Parameters		**Physical Parameters**	
d_B	D	D_{HL}	I
E_L	I	K_H	D
k_L	I		
ϵ_g	D		
Reaction Parameters		**Operation Parameters**	
k_H''	I	d_R	I
U	I	f	D
$-\alpha$	D	$u_g{}^i$	D
		wf_{Fe}	I
		$L(1-\epsilon_g)$	I
Dimensionless Parameters			
Pe_L	D		
St_d	I		
St_k	I		

(1) "D" denotes a decreasing value and "I" denotes an increasing value of a parameter $(1-X_H{}^e)_{AD}/(1-X_H{}^e)_{NM}$.

FIGURE 43

EFFECT OF AXIAL LIQUID MIXING ON BSU F-T REACTOR PERFORMANCE

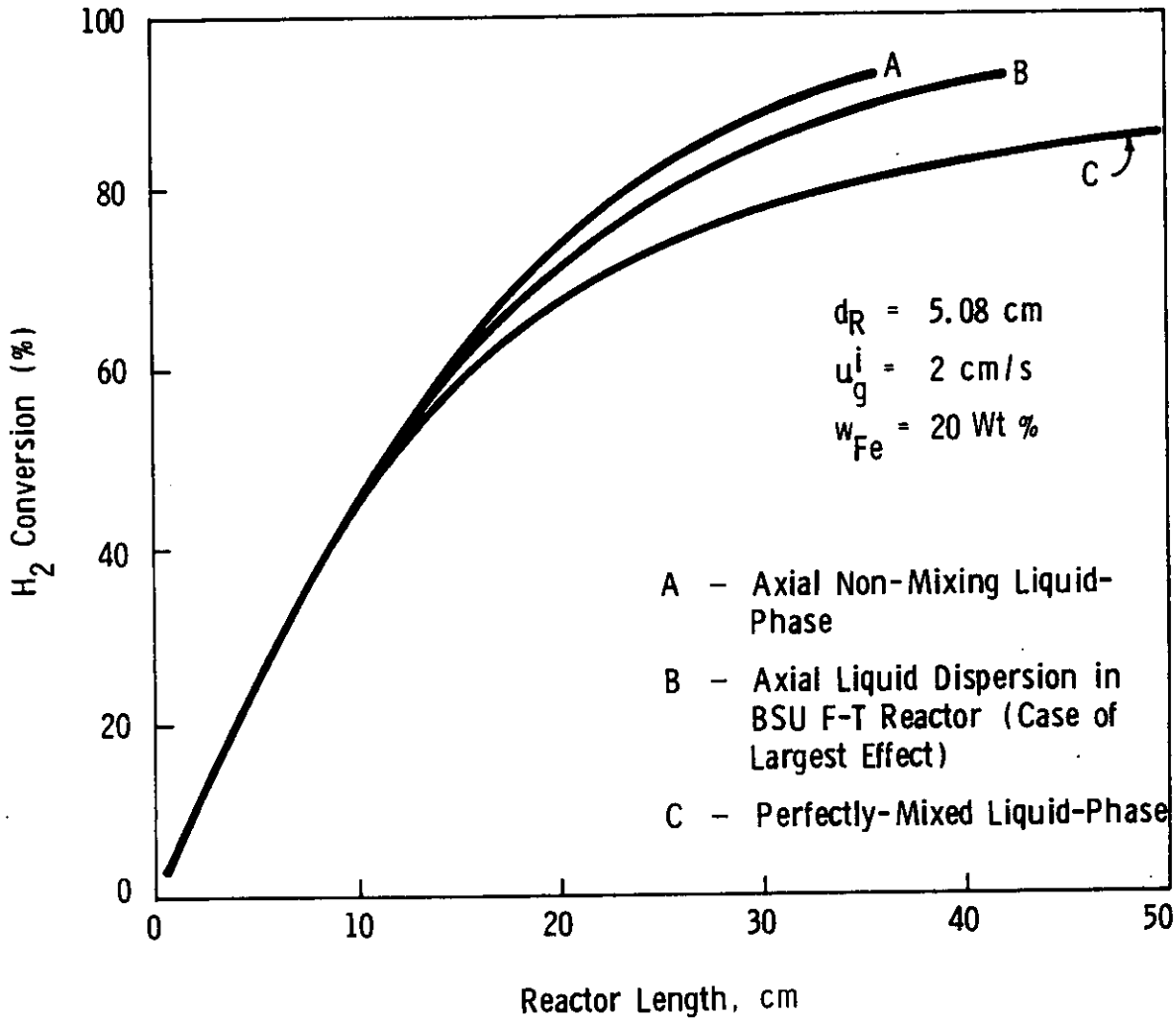

the largest effect case is, as expected, enveloped on both sides by those of the non-mixing and the perfectly-mixed liquid cases. The perfectly-mixed liquid case deviates substantially from the largest effect case; while the deviation between the non-mixing liquid phase and the largest effect case is small to moderate. In the latter comparison, the reactor length required to achieve a 90% conversion is about 15% longer than that estimated using the non-mixing liquid phase approximation. In conclusion, the liquid-phase axial mixing effect is small and shall be included in model calculations only if very accurate results are desired.

In a large-scale F-T reactor, the effect of the liquid-phase axial mixing is expected to become larger because of less hindrance from the reactor wall on the liquid movement. However, there are three factors that greatly complicate this issue. The first factor is that, in a large-scale reactor, the operational gas velocity, whose upper bound is determined by the existence of the gas-liquid slug flow in smaller reactors, become substantially higher. With a higher gas velocity, the effect of the liquid-phase axial dispersion becomes less. The second factor is that a large-scale reactor will contain a large number of cooling tubes in the reactor to remove reaction heat. The existence of the cooling tubes will provide the surfaces that hinder the liquid movement and reduce the liquid-phase axial mixing. The last factor is the possible existence of the churn-turbulent flow-region in a large-scale high gas velocity reactor (Deckwer, et al., 1982a). More studies, particularly non-reacting flow model experiments, are essential in understanding the hydrodynamic behavior of such systems. In the following, a preliminary study was done using the actual operational data of the 155 cm inside diameter and 8.6 m height Rheinpreussen-Koppers demonstration reactor.

To maximize the effect of the calculated liquid-phase axial mixing, the upper bound of the liquid-phase hydrogen diffusivity and the lower bound of the hydrogen solubility coefficient were adopted in the calculation. Assuming that the hydrodynamic description used in the current mathematical model can be applied to this case study, an effective reactor diameter must be estimated to account for the existence of the vertical cooling tubes. One may define this effective reactor diameter as the hydraulic diameter of the free flow area, i.e., the equivalent circular diameter that gives the same perimeter to flow area ratio. The hydraulic diameter of this reactor is 25.4 cm. However, another effective reactor diameter defined as the equivalent circular diameter that gives the same free flow area has also been proposed. This equivalent diameter is 129 cm, which is substantially different from the hydraulic diameter. It is not clear which definition gives a better representation of the actual phenomenon. The effective reactor diameter may lie between these two diameters. In Figure 44, calculated results based on these two diameters are shown together with the two

FIGURE 44

EFFECT OF AXIAL LIQUID MIXING ON LARGE-SCALE F-T REACTOR PERFORMANCE

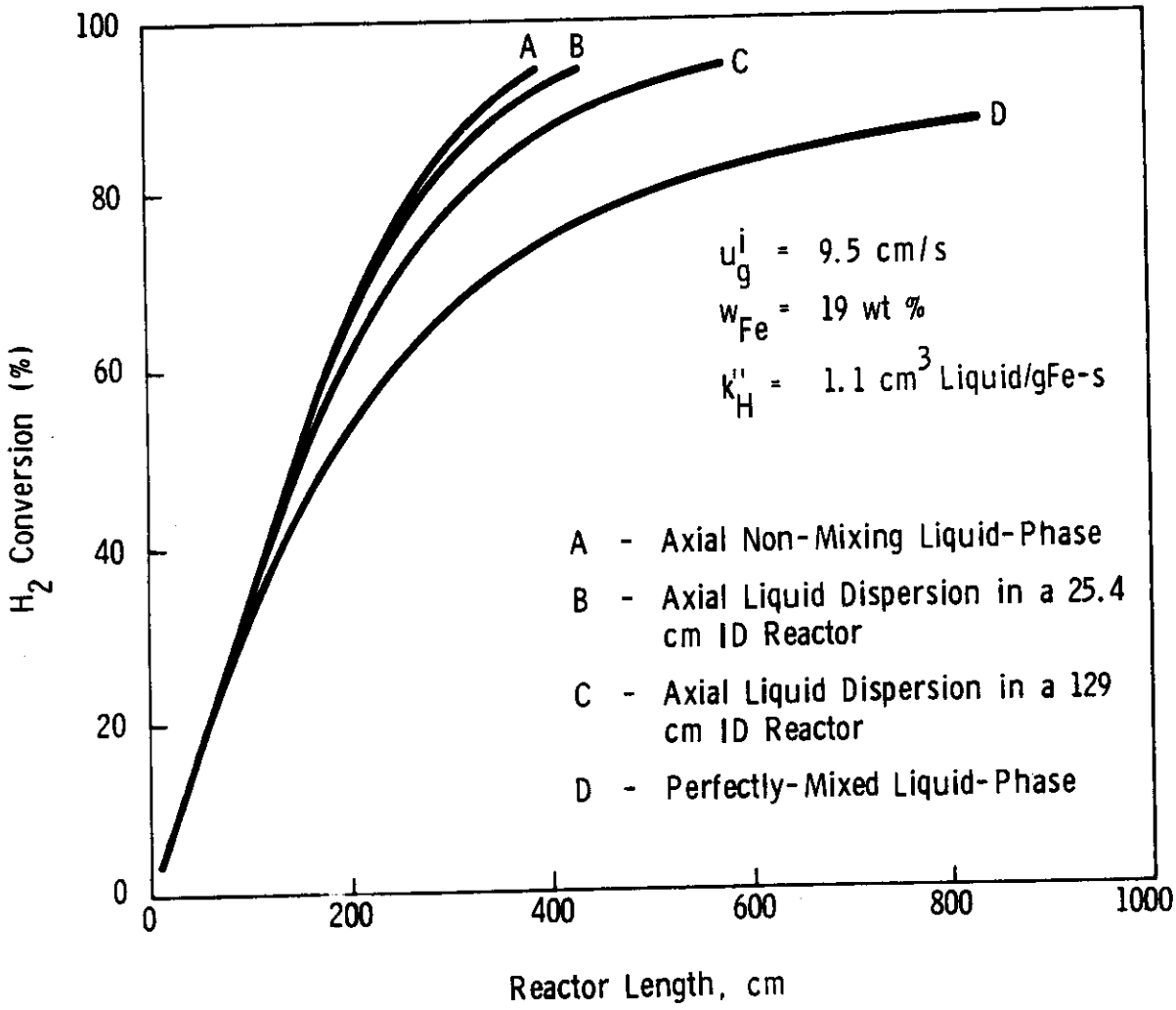

extreme cases of the non-mixing and the perfectly-mixed liquid. Using the hydraulic diameter as the effective reactor diameter results in about 10% longer reactor than that required in the non-mixing liquid case, while using the free-flow-area diameter results in about 50% longer reactor. This reactor performance is far from the perfectly-mixed liquid-phase case. Note that if the hydraulic diameter is the proper effective reactor diameter for accounting for the effect of vertical cooling tubes, the reactor scale-up problem will become very simple.

2. Multi-Component Model

In the previous subsection, the F-T bubble-column mathematical model was constructed based on a single reactant component (H_2), and a single first-order F-T kinetic expression. This simple approach allows a quick way of solving the associated mathematical equations. However, these simple-minded assumptions give approximate descriptions of the transport phenomena and the kinetics of the system. For example, since the H_2 diffusivity is substantially higher than the diffusivities of CO and other components, the mass transfer resistance in a single-component model is less than that in a multi-component system. Furthermore, first-order kinetics give an overly optimistic prediction of the H_2+CO conversion at high conversions, where the kinetics approach second-order according to Dry (1976). The multi-component mathematical model also includes a separate water-gas shift reaction which describes a kinetic conversion of CO to H_2 using the H_2O formed in the F-T reactions.

a. Estimate of Kinetic Parameters From A Set of Published F-T Column Data

A set of literature data from a bench-scale F-T bubble-column was used to estimate the kinetic parameters of a precipitated Fe-catalyst (Koelbel and Ralek, 1980). The operation conditions from this data set are summarized in Table 34. In addition to these conditions, the solubilities and diffusivities of all four components were required and estimated either from experimental data or correlation equations as summarized in Table 28. The correlations used to calculate the liquid-side mass transfer coefficient, gas holdup, and liquid density and viscosity were the same as those used in Subsection VII.D.1 (see Table 27). Values of bubble size, catalyst solid density, iron fraction in the catalyst, and molar contraction factor were also the same as those used in the previous section. The parameters are summarized in Table 35 as the base case.

The numerical scheme used to estimate the kinetic parameters was the method of parametric regression, minimizing the following target function:

$$(1 - (X_{H_2+CO})_{calc}/(X_{H_2+CO})_{exp})^2 + (1-U_{cal}/U_{exp})^2 \qquad (39)$$

Table 34

Bench-Scale Bubble-Column Data for Estimating Kinetics of a Precipitated Fe-Catalyst[1]

$T = 266°C$	$f = 0.67$
$P = 1.1$ MPa	$f_{Fe} = 0.67$
$u_g^i = 3.5$ cm/s	$U^e = 0.65$
$L = 350$ cm	$X_{H2+CO} = 88\%$
$w_{Fe} = 10\%$	$m = 2.24$[2]

[1] Koelbel and Ralek (1980).

[2] Probstein and Hicks (1982).

Table 35

Parameters and Their Ranges Adopted In F-T Multi-Component Model Calculations

Operation Parameters	Base Case	Range
T (°C)	265	
u_g^i (cm/s)	4	2-6
w_{Fe}	.10	.05-.15
f	.7	.6-.8
Reaction Parameters		
K_1(cm^3 liquid/s-gFe)	2.09	
k_2 (cm^3 liquid/s-gFe)	1.52	
k_3	.756	
k_4	34.7	
α	-.5	
m	2.24(1)	
Physical Parameters		
K (cm^3 liquid/cm^3 gas)	4.55-3.70-1.78-1.18(2)	
D_L (cm^2/s) x 10^{-4}	1.86-.288-.256-.441(2)	
ρ_L (g/cm^3 liquid)	.666	
μ_L (g/cm-s)	.0225	
ρ_s (g/cm^3 solid)	5.2	
f_{Fe}	.67	
Hydrodynamic Parameters		
d_B (cm)	.07	
ϵ_g	$.053(u_g)^{1.1}$	
k_L (cm/s) x 10^{-2}	3.15-.909-.840-1.21(2)	

(1)Probstein and Hicks (1982).
(2)For H_2-CO-CO_2-H_2O, respectively.

The convergence criterion was that this target function was less than 10^{-5}. The resulting kinetic parameters are included in Table 35. This set of kinetic parameters was adopted in the following calculations.

b. Comparison of Single Component and Multi-Component Models

Due to interaction of the water-gas shift and Fischer-Tropsch reaction, the nonlinear kinetics (see above) and the different diffusivities of H_2 and CO, certain features predicted by the multi-component model could not be exhibited by the single component models.

The major differences between the predictions of these two mathematical models are:

- The reactor length required for given H_2+CO conversion is significantly longer at high conversions than that predicted by the single component model.
- The mass transfer limitations are significantly larger (due to CO) than predicted by the single component model.
- The H_2/CO ratio in the liquid phase is larger than that in the gas phase and can be significantly larger than the feed H_2/CO ratio.

Because of the complex kinetic expression used in the current improved model, it was not straightforward to compare the current kinetic constants with the single constant obtained in the previous single-component (H_2) kinetic expression. From Equation (29), the rate expression for the F-T reaction will be reduced to the simple first order kinetic expression previously used when $[CO] >> k_3[H_2O]$. This occurs at the entrance portion of a F-T bubble-column when a dry synthesis gas is used. However, the rate becomes minute when [CO] and $[H_2]$ become small. This description indicates that the H_2+CO conversion rate at the entrance of a bubble-column is higher than that which is predicted using the first-order model. Nevertheless, when the synthesis gas conversion proceeds, the conversion rate approaches second-order kinetics, and the rate becomes significantly lower. This observation is clearly illustrated in Figure 45. The constants k_2 and k_4 describe the rate of the water-gas shift reaction (Equation (31), which significantly affects the H_2, CO, H_2O, and CO_2 concentrations along the reaction path. The estimated equilibrium constant k_4 (34.7) matches exactly the experimental equilibrium constant given by Newsome (1980).

FIGURE 45

COMPARISON OF MULTI-COMPONENT F-T BUBBLE-COLUMN MATHEMATICAL MODEL WITH SINGLE-COMPONENT MODEL

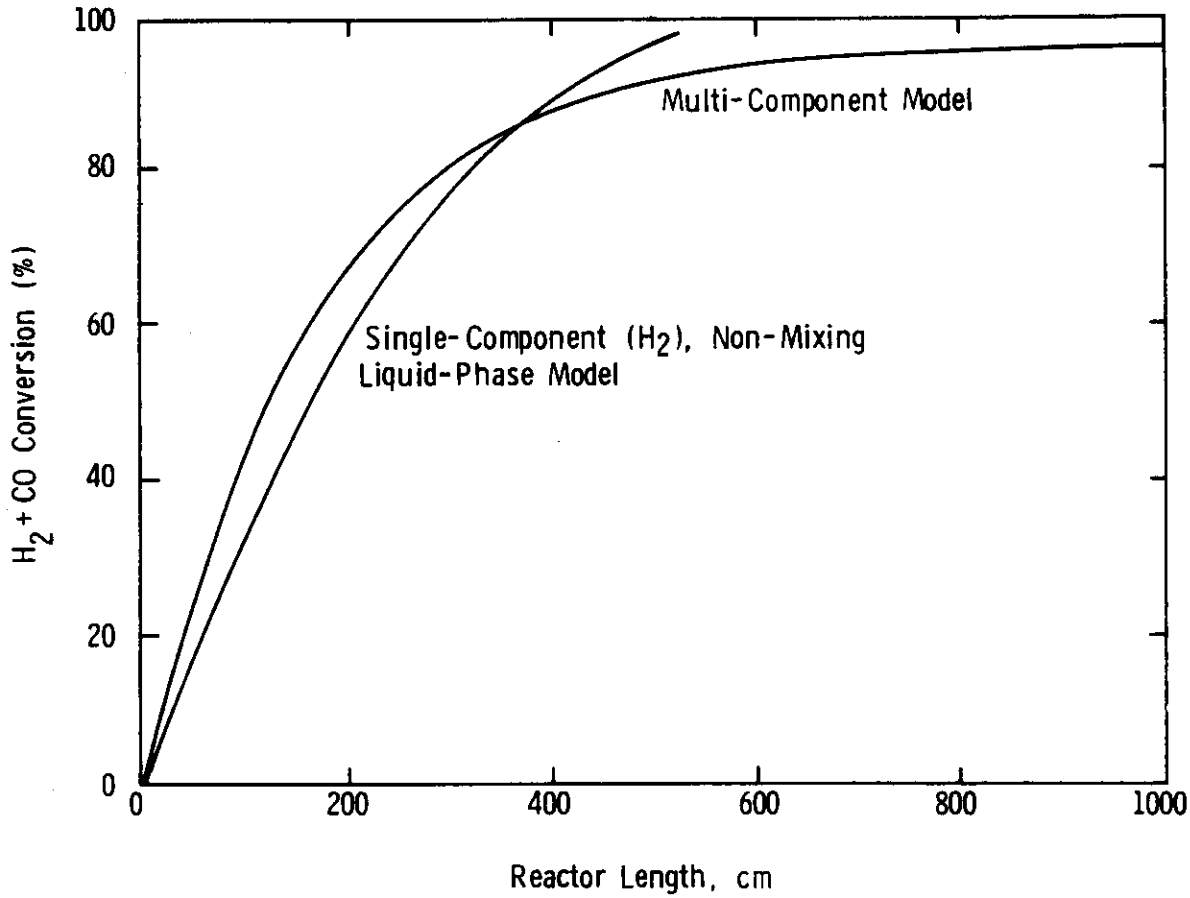

Figure 46 shows the variation of H_2, CO, CO_2, and H_2O concentrations in both the gas- and the liquid phase along the bubble-column. Note that CO_2 concentration increases quickly along the column because the water-gas shift reaction favors the CO_2 formation under the given conditions. Also, the H_2O concentration varies only a little after the entrance portion of the column since the rate of its dissipation by the water-gas shift reaction is approximately balanced by its rate of formation due to the F-T reaction. Figure 47 shows the variation of the F-T and water-gas shift reaction rates along the column. The F-T rate decreases quickly along the reaction path. Figure 48 shows the H_2/CO ratios in both the gas- and liquid-phase along the column height. Along most of the column, the H_2/CO ratio in the liquid-phase is higher than that of the gas-phase because the H_2 mass transfer coefficient is substantially larger than that of the CO. It is interesting to see that the H_2/CO ratio has a minimum, and that the water-gas shift reaction rate and the H_2O concentrations have a maximum along the column height. All these phenomena can be properly explained by the existence of the water-gas shift reaction.

The question of how important the mass transfer resistance is across the gas-liquid interface becomes more complex for the multi-component system. Nevertheless, a single component (H_2) model may under-predict a gas-liquid mass transfer resistance, since H_2 has the highest diffusivity (about 6.5 times that of the CO) among the four components used in the current model.

c. Parametric Study

Parametric studies were performed using the multi-component mathematical model and the parameters listed in Table 35. The major results are:

- Varying superficial gas velocities (2, 4, 6 cm/s) and Fe-catalyst loadings in the reactor slurry (5, 10, 15 wt %) has a large effect on the F-T bubble-column performance. However, the effect of increasing the catalyst loading from 10 to 15 wt % is considerably less than that of increasing it from 5 to 10 wt%.

- The effect of varying the feed H_2/CO ratio (.6, .7, and .8) on the F-T bubble-column performance is not significant except in the high H_2+CO conversion region. The reactor exit gas H_2/CO ratio also increases significantly with increasing feed H_2/CO ratios when the conversion is high. This may somewhat affect the catalyst aging and the methane formation rate, both of which depend on the H_2/CO ratio in the gas phase.

FIGURE 46

PREDICTED AXIAL CONCENTRATION PROFILES IN F-T BUBBLE-COLUMN
(Conditions of Table 34)

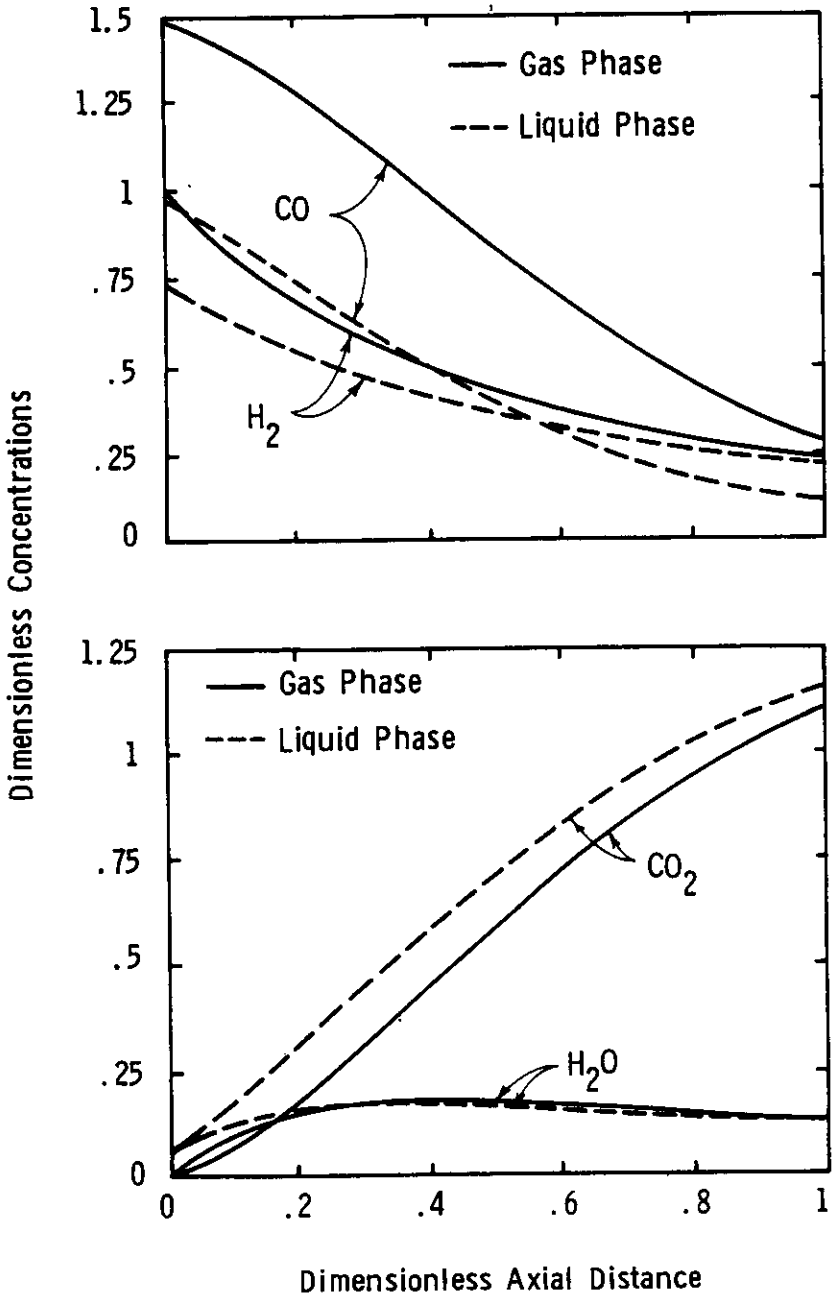

FIGURE 47

PREDICTED REACTION RATES
(Conditions of Table 34)

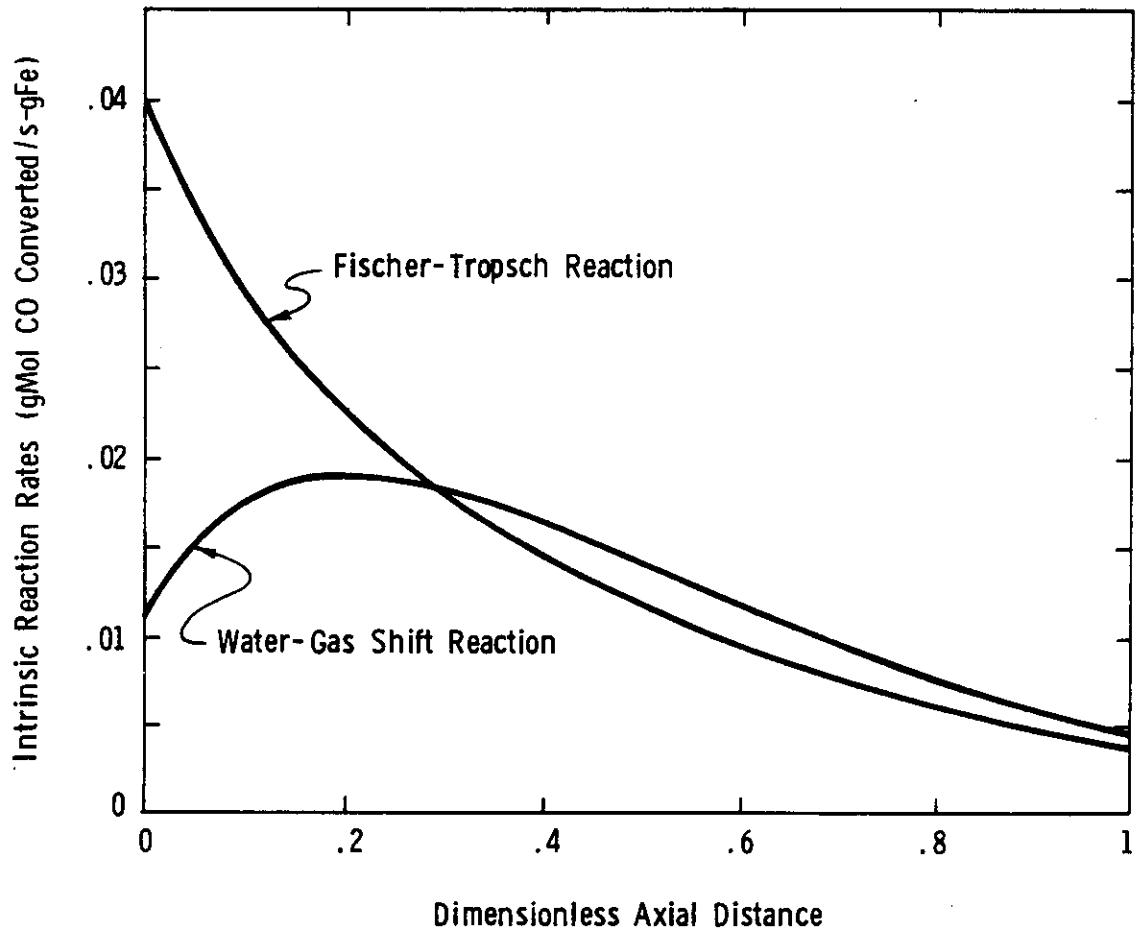

FIGURE 48

PREDICTED H_2/CO RATIO
(Conditions of Table 34)